

Intensity noise properties of quantum cascade lasers

Tobias Gensty and Wolfgang Elsäßer

*Institute of Applied Physics, Darmstadt University of Technology, Schlossgartenstrasse 7,
D-64289 Darmstadt, Germany*

tobias.gensty@physik.tu-darmstadt.de

Christian Mann

*Fraunhofer-Institut für Angewandte Festkörperphysik (IAF), Tullastrasse 72, D-79108
Freiburg, Germany*

Abstract: We present investigations of the the relative intensity noise (RIN) of a quantum cascade laser (QC) laser in continuous wave operation. We analyze the intensity noise properties in terms of the relative intensity noise (RIN). In contrast to conventional interband semiconductor diode lasers we obtain a different scaling behavior of RIN with increasing optical output power for QC lasers. From a semiclassical noise model we find that this result is due to the cascaded active regions each incorporating three laser levels, and is therefore a particular feature of QC lasers.

© 2005 Optical Society of America

OCIS codes: (140.5960) Semiconductor lasers; (270.2500) Fluctuations, relaxations, and noise; (140.3070) Infrared and far-infrared lasers; (999.9999) Quantum cascade lasers

References and links

1. F. T. Arecchi, *Laser Handbook* (North-Holland, Amsterdam, 1972).
2. H. Haken, *Laser Theory Vol. XXXV/2C. Encyclopedia of Physics* (Springer-Verlag, Berlin, 1970).
3. J. Woerdman, M. V. Exter, and N. V. Druten, "Quantum noise of small lasers," *Adv. in Atomic, Molecular, and Optical Physics* **47**, 205-248 (2001).
4. H. Hofmann and O. Hess, "Coexistence of thermal noise and squeezing in the intensity fluctuations of small laser diodes," *J. Opt. Soc. Am. B* **17**, 1926-1933 (2000).
5. J. Poizat and P. Grangier, "Quantum noise of laser diodes," *J. Mod. Optics* **47** 2841-2856 (2000).
6. J.-L. Vey, C. Degen, K. Auen, and W. Elsäßer, "Quantum noise and polarization properties of vertical-cavity surface-emitting lasers," *Phys. Rev. A* **60**, 3284-3295 (1999).
7. Y. Yamamoto, "AM and FM quantum noise in semiconductor-lasers. 1. Theoretical-analysis," *IEEE J. Quantum Electron.* **QE-19**, 34-46 (1983).
8. Y. Yamamoto, S. Saito, and T. Mukai, "AM and FM quantum noise in semiconductor-lasers. 2. Comparison of theoretical and experimental results for AlGaAs lasers," *IEEE J. Quantum Electron.* **QE-19**, 47-58 (1983).
9. K. Vahala and A. Yariv, "Semiclassical theory of noise in semiconductor-lasers. 1.," *IEEE J. Quantum Electron.* **QE-19**, 1096-1101 (1983).
10. K. Vahala and A. Yariv, "Semiclassical theory of noise in semiconductor-lasers. 2.," *IEEE J. Quantum Electron.* **QE-19**, 1102-1109 (1983).
11. Y. Li and M. Xiao, "Generation and applications of amplitude-squeezed states of light from semiconductor diode lasers," *Opt. Express* **2**, 110-117 (1998), <http://www.opticsexpress.org/abstract.cfm?URI=OPEX-2-3-110>
12. Y. Yamamoto, S. Machida, and R. H. Richardson, "Photon number squeezed states in semiconductor-lasers," *Science* **255**, 1219-1224 (1992).
13. B. C. Buchler, E. H. Huntington, C. C. Harb, and T. C. Ralph, "Feedback control of laser intensity noise," *Phys. Rev. A* **57**, 1286-1294 (1998).
14. T. Gantsog, G. M. Meyer, M. O. Scully, and H. Walther, "Dynamic control of micromaser and laser emission from driven three-level atoms," *Opt. Commun.* **124**, 579-594 (1996).
15. M. Orszag, S. Y. Zhu, J. Bergou, and M. O. Scully, "Noise-reduction, lasing without inversion, and pump statistics in coherently prepared lambda quantum-beat media," *Phys. Rev. A* **45**, 4872-4878 (1992).

16. K. M. Gheri and D. F. Walls, "Sub-shot noise lasers without inversion," *Phys. Rev. Lett.* **68**, 3428-3431 (1992).
17. J. Faist, F. Capasso, D. L. Sivco, C. Sirtori, A. L. Hutchinson, and A. Y. Cho, "Quantum cascade laser," *Science* **264**, 553-556 (1994).
18. C. Mann, Q. K. Yang, F. Fuchs, W. Bronner, R. Kiefer, K. Khler, H. Schneider, R. Korrman, H. Fischer, T. Gensty, and W. Elsässer, "Quantum Cascade Lasers for the mid-infrared spectral range: Devices and applications," in B. Kramer, ed., *Adv. in Solid State Phys.* **43**, 351-368 (Springer, Berlin, Heidelberg, 2003).
19. J. Faist, A. Tredicucci, F. Capasso, C. Sirtori, D. L. Sivco, J. N. Baillargeon, A. L. Hutchinson, and A. Y. Cho, "High-power continuous-wave quantum cascade lasers," *IEEE J. Quantum Electron.* **QE-34**, 336-343 (1998).
20. C. Mann, Q. K. Yang, F. Fuchs, W. Bronner, and K. Köhler, "Continuous-wave operation of 5 μm quantum cascade lasers with high-reflection coated facets," *Electron. Lett.* **39**, 1590-1592 (2003).
21. J. S. Yu, S. Slivken, A. Evans, J. David, and M. Razeghi, "High-power continuous-wave operation of a 6 μm quantum-cascade laser at room temperature," *Appl. Phys. Lett.* **82**, 3397-3399 (2003).
22. The quantum cascade laser structure has been grown by Fraunhofer-Institut für Angewandte Festkörperphysik (IAF), Tullastrasse 72, D-79108 Freiburg, Germany.
23. R. Köhler, C. Gmachl, A. Tredicucci, F. Capasso, D. L. Sivco, S.-N. G. Chu, and A. Y. Cho, "Single-mode tunable, pulsed, and continuous wave quantum-cascade distributed feedback lasers at $\lambda \cong 4.6 - 4.7 \mu\text{m}$," *Appl. Phys. Lett.* **76**, 1092-1094 (2000).
24. H.-A. Bachor, *A Guide to Experiments in Quantum Optics* (WILEY-VCH, Weinheim, New York, Chichester, Brisbane, Singapore, Toronto, 1998).
25. F. Capasso, R. Paiella, R. Martini, R. Colombelli, C. Gmachl, T. L. Myers, M. S. Taubman, R. M. Williams, C. G. Bethea, K. Unterrainer, H. Y. Hwang, D. L. Sivco, A. Y. Cho, A. M. Sergent, H. C. Liu, and E. A. Whittaker, "Quantum cascade lasers: Ultra-speed operation, optical wireless communication, narrow linewidth, and far-infrared emission," *IEEE J. Quantum Electron.* **QE-38**, 511-532 (2002).
26. T. Gensty, J. von Staden, and W. Elsässer, "Investigations on the generation of light with sub-shot intensity noise with quantum cascade lasers," in *Fluctuations and Noise in Photonics and Quantum Optics II*, P. Heszler, D. Abbott, J. R. Gea-Banacloche, and Ph. R. Hemmer, eds., *Proc. SPIE* **5468**, 191-197 (2004).
27. T. Mukai and Y. Yamamoto, "AM Quantum noise in 1.3 μm InGaAsP lasers," *Electron. Lett.* **20**, 28-29 (1984).
28. I. Joindot, "Measurements of relative intensity noise (RIN) in semiconductor-lasers," *J. Phys. III* **2**, 1591-1603 (1992).
29. D. Kuchta, J. Gamelin, J. D. Walker, J. Lin, K. Y. Lau, and J. S. Smith, "Relative intensity noise of vertical cavity surface emitting lasers," *Appl. Phys. Lett.* **62**, 1194-1196 (1993).
30. H. Fischer and M. Tacke, "High-frequency intensity noise of lead-salt diode-lasers," *J. Opt. Soc. Am. B* **8**, 1824-1830 (1991).
31. H. Haug, "Quantum-mechanical rate equations for semiconductor lasers," *Phys. Rev.* **184**, 338-348 (1969).
32. F. Koyama, K. Morito, and K. Iga, "Intensity noise and polarization stability of GaAlAs-GaAs surface emitting lasers," *IEEE J. Quantum Electron.* **QE-27**, 1410-1416 (1991).

From the early days of laser science there has been a perpetual drive to understand the noise, the fluctuations of laser light [1, 2]. With every advent of a new laser structure there has been a renaissance of this demand to explore and to understand the intensity noise, both from the theoretical and the experimental point of view (see e.g. Ref. [3–10]). Furthermore, with the understanding of the intensity noise properties the control and the reduction of the laser noise, even below the standard quantum limit, became possible [11–16]. With the advent of the youngest semiconductor laser, the quantum cascade (QC) laser [17], the question of intensity noise performance of this unipolar intersubband laser source arose once more again. Do QC lasers behave differently from other semiconductor interband lasers due to their particular level scheme? In this letter we shall answer this question experimentally and theoretically. We will demonstrate that QC lasers have a different power dependence of their intensity noise on the optical power which is due to the effective cascaded three-level scheme they represent. The answer to this question is also of interest for the application of QC lasers as a light source for spectroscopic systems and for optical free-space data communication systems, because laser noise may limit the sensitivity of absorption spectroscopy as well as the bandwidth and the transmission range of optical free-space data links [18].

QC lasers are unipolar intersubband lasers in which the laser transition occurs between quantized states of the conduction band. The typical conduction band profile together with the resulting energy levels representing the three-level laser scheme is depicted in Fig. 1. The electrons

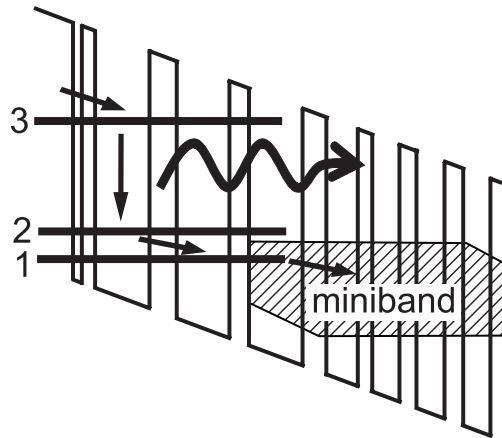


Fig. 1. Schematic conduction band profile of one gain stage of a 3-level QC laser. Also indicated is the electron transport (arrows) and photon emission (wavy arrow) due to the laser transition between level 3 and 2.

are injected into level 3 which acts as the upper laser level. The laser transition occurs between level 3 and level 2. In order to obtain population inversion, the electrons have to be efficiently extracted from the lower laser level (level 2). This is achieved by using the resonant electron-phonon scattering process. Therefore, level 2 and level 1 are designed in a way that the energy difference between these two levels is close to the energy of the longitudinal optical phonon. This results in a much shorter lifetime of the lower laser level than the lifetime of the upper laser level (c.f. Table 1) which is a necessary condition in order to obtain population inversion for the laser transition. Finally, the electrons are extracted from level 1 into the adjacent miniband. From there, the electrons reach the injector of the subsequent three-level laser system and are injected into the the upper laser level again. Hence, Fig. 1 represents one single gain stage incorporated into the active region of a QC laser. Typically, the active region of a state-of-the-art QC laser consists of a period of Z cascaded gain stages and electron injectors where Z is typically $\sim 25 - 35$ [19–21].

The investigated device [22] is based on strain-compensated GaInAs/AlInAs employing a triple quantum well active region as published in Ref. [23]. Twenty-five periods of alternating active regions and injectors were grown on InP substrate by molecular beam epitaxy. After that InP was grown by low-temperature metal-organic vapor phase epitaxy serving as upper waveguide and contact layer [20]. A $10 \times 1000 \mu\text{m}^2$ device mounted substrate side down with uncoated facets is investigated for which a maximum continuous wave (cw) operating temperature of 135 K was determined. At 88 K, the laser exhibits a threshold current of $I_{thr} = 195 \text{ mA}$ and the laser emission is observed at a wavelength of $4.98 \mu\text{m}$ in a single longitudinal mode. The operating voltage is approximately 10 V and the maximum optical power is 19 mW per facet at an injection current of $I = 400 \text{ mA}$.

The experimental setup for the investigations of the intensity noise properties is a direct detection scheme [24] and is depicted in Fig. 2. The QC laser is operated using a 24 V battery current source. The emitted light is collected by a $f/1.6$ elliptical mirror and focused onto a peltier-cooled HgCdZnTe photovoltaic detector (Vigo, PDI-2TE-10.6) with an active area of $1 \times 1 \text{ mm}^2$ and a bandwidth of $\sim 350 \text{ MHz}$. Special care has been taken in order to avoid optical feedback in the experimental setup. The detected photocurrent is separated into the alternating current (AC) and the direct current (DC) by a so called “Bias-Tee” (Picosecond Pulse Labs,

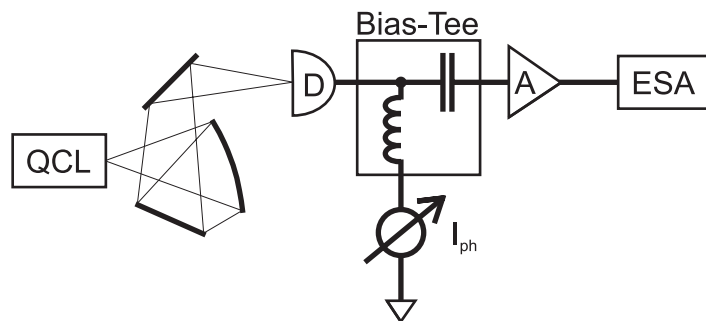


Fig. 2. Scheme of the experimental setup. The emitted light of the quantum cascade laser (QCL) is collected by an elliptical mirror and focused onto the photovoltaic detector (D). The detected signal is split into the AC current and DC current by a Bias-Tee. The AC part is analyzed by an electrical spectrum analyzer (ESA) after amplification using a low noise amplifier (A). The photocurrent I_{ph} is measured in the DC part of the signal.

model 5546). The AC part of the signal accounts for the fluctuations of the laser intensity. It is analyzed by an electrical spectrum analyzer (ESA, HP8568B) after amplification using a 20 dB low noise amplifier (Mini-Circuits, ZFL-1000LN). The DC part of the signal gives the photocurrent I_{ph} which is proportional to the mean optical intensity. The intensity fluctuations are characterized by the relative intensity noise (RIN) which is defined as the ratio of the mean value of the optical intensity fluctuation δP squared to the mean optical power P_0 squared at a specified frequency ω in a 1 Hz bandwidth:

$$RIN(\omega) = \frac{\langle \delta P^2 \rangle}{P_0^2}. \quad (1)$$

This ratio can be expressed as the ratio of the detected electrical powers, thus

$$RIN(\omega) = \frac{S_P(\omega)}{BG I_{ph}^2 R}, \quad (2)$$

where the spectral noise power $S_P(\omega)$ is the difference between the measured spectral noise power of the signal of the illuminated detector and the spectral dark noise power at the frequency ω . The mean electrical power of the detected signal is given by $I_{ph}^2 R$. Here, R is the impedance of the amplifier and I_{ph} is the photocurrent of the detected signal given by the difference between the photocurrent of the illuminated detector and the dark current, respectively. The resolution bandwidth B of the ESA gives the normalization to the 1 Hz bandwidth and G accounts for the gain of the amplifier.

The experimentally determined RIN of the QC laser in cw operation is depicted in Fig. 3 as a function of the emitted optical power P_0 measured in the low frequency limit [3, 5, 8] at a frequency ω of 40 MHz. The frequency of 40 MHz is much smaller than the relaxation oscillation frequency which is typically in the order of several GHz for QC lasers [25]. RIN of the QC laser decreases with increasing optical power from $-124.5 \text{ dB}\cdot\text{Hz}^{-1}$ at $P_0 = 0.3 \text{ mW}$ to $-155.0 \text{ dB}\cdot\text{Hz}^{-1}$ at $P_0 = 18.6 \text{ mW}$. The measured value of the RIN of $-155.0 \text{ dB}\cdot\text{Hz}^{-1}$ is $\sim 2.5 \text{ dB}$ above the standard quantum noise limit which we have verified using different shot noise sources [26]. The experimental data can be fitted according to a simple power-law $RIN \propto P_0^{-\gamma}$, with $\gamma = 2.18 \pm 0.1$. The same measurement at a frequency of 50 MHz yields $\gamma = 1.9 \pm 0.2$. Thus, we find that in QC lasers RIN decreases with increasing optical power with

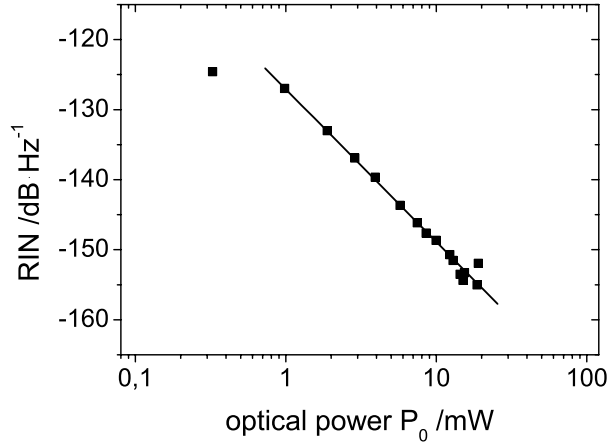


Fig. 3. Experimentally determined RIN as a function of the emitted optical power of the investigated QC laser in cw-operation at a heat sink temperature of $T = 88$ K. The RIN is measured at a frequency of 40 MHz. The solid line depicts the least-square fit to the experimental data.

$\gamma \approx 2.1$. Compared to these results, for interband semiconductor diode lasers, $\gamma = 3$ has been determined experimentally for edge emitting lasers [27, 28], vertical-cavity surface emitting lasers (VCSELs) [29], and for lead-salt diode lasers [30], as well as theoretically based on a small signal rate equation analysis for a 2-level laser system in which the laser transition is realized by an electron-hole recombination between the conduction band and the valence band [31, 32]. Thus, our experimental finding of $\gamma \approx 2$ demonstrates that QC lasers have a different scaling behavior in the dependence of their intensity noise on the optical power than interband diode lasers.

In order to get a better understanding of the intensity noise properties of QC lasers we develop a semiclassical noise model based on three-level rate equations for QC lasers. Three equations for the level populations N_3 , N_2 , N_1 in level 3, 2 and 1, respectively, and one for the photons P result in the case of 25 gain stages in a set of 100 equations, which can be reduced to four equations by summing over all gain stages incorporated into the active region. Hence, we obtain the rate equations describing effectively the whole cascaded structure of a QC laser:

$$\frac{dN_3}{dt} = \frac{I_{in}}{q} - \frac{N_3}{\tau_{32}} - \frac{N_3}{\tau_{31}} - g(N_3 - N_2)P, \quad (3)$$

$$\frac{dN_2}{dt} = \frac{N_3}{\tau_{32}} - \frac{N_2}{\tau_{21}} + g(N_3 - N_2)P, \quad (4)$$

$$\frac{dN_1}{dt} = \frac{N_3}{\tau_{31}} + \frac{N_2}{\tau_{21}} - \frac{I_{out}}{q}, \quad (5)$$

$$\frac{dP}{dt} = Zg(N_3 - N_2)P + Z\beta \frac{N_3}{\tau_e} - \frac{P}{\tau_P}. \quad (6)$$

where q is the electron charge, I_{in} is the current into level 3 and I_{out} is the current out off level 1 into the adjacent miniband. The phonon scattering times τ_{31} , τ_{32} , and τ_{21} account for non-

radiative losses of carriers due to electron-phonon scattering, $\tau_e = (\tau_{31}^{-1} + \tau_{32}^{-1})^{-1}$ denotes the electron lifetime of the carriers in level 3, and τ_p is the photon lifetime. Since we assume that $I_{out}^n = I_{in}^{n+1}$ where I_{out}^n and I_{in}^{n+1} are the currents out off level 1 of the n -th gain stage and into level 3 of the $(n+1)$ -th gain stage, respectively, it follows that $I_{in} = I_{out}$, and hence, I_{in} is the effective current through all gain stages. In Eq. (6), $g(N_3 - N_2)$ denotes the gain of one gain stage with g being the differential gain parameter, β is the spontaneous emission factor, and Z is the number of cascaded gain stages. Performing a small signal analysis of the rate equations and adding Langevin noise sources we are able to obtain an analytical expression for RIN in the frequency domain. We find that by using realistic laser parameters (c.f. Table 1) RIN can be expressed as

$$RIN(\omega) = R_{PP}(\omega) + R_{33}(\omega) \quad (7)$$

where R_{PP} and R_{33} denote the major contributions to the total RIN and represent the individual contributions of the Langevin noise sources. The Langevin noise sources are defined to exhibit a white noise behavior. Hence, the average of the Langevin noise sources vanishes, $\langle F_P \rangle = \langle F_3 \rangle = 0$, but the correlations of the Langevin noise sources are non-zero. They are given by

$$\langle F_P F_P \rangle = 2Z \left(\beta \frac{N_3}{\tau_e} + gN_3P \right) \equiv 2D_{PP} \quad (8)$$

$$\langle F_3 F_3 \rangle = 2 \left(\frac{N_3}{\tau_{31}} + \frac{N_3}{\tau_{32}} + gN_3P \right) \equiv 2D_{33}. \quad (9)$$

By using Eqs. 8 and 9 the individual contributions to the total RIN, R_{PP} and R_{33} , can be expressed as

$$R_{PP}(\omega) = 2D_{PP}f_P(\omega) \quad (10)$$

$$R_{33}(\omega) = 2D_{33}f_3(\omega) \quad (11)$$

where $f_P(\omega)$ and $f_3(\omega)$ denote the individual terms resulting from the solution of the small signal rate equations with respect to the small signal photon number $|p(\omega)|^2$. We find from Eq. (7) that the main noise sources for R_{PP} and R_{33} are the spontaneous emission and non-radiative losses of carriers out off level 3 due to electron-phonon scattering, respectively. Thus, the intensity noise of 3-level QC lasers comprises two noise sources, the spontaneous emission and electron-phonon scattering losses. In contrast, the intensity noise of interband diode lasers is dominated only by the spontaneous emission.

The calculated RIN for a QC laser incorporating 25 gain stages at a frequency of 40 MHz as a function of the optical power is depicted in Fig. 4. The laser parameters used for the calculations are shown in Table 1. The dashed and dotted lines represent the individual contributions R_{33} and R_{PP} adding up to the total RIN as defined by Eq. (7). Also shown is the experimental RIN of Fig. 3 for comparison. We find good agreement between the calculated and the experimentally obtained results. In general, R_{PP} and R_{33} do not follow a power-law. However, in the investigated power regime, i.e. for optical powers $P_0 < 20$ mW, R_{PP} and R_{33} can be approximated by a power-law with scaling parameters γ_P and γ_3 , namely $R_{PP} \propto P_0^{-\gamma_P}$ and $R_{33} \propto P_0^{-\gamma_3}$. We find that $\gamma_P = 2.8$, whereas $\gamma_3 = 1.8$. Thus, the spontaneous emission results in a dependence of RIN of QC lasers on the optical power scaling with $\gamma = 2.8$, and non-radiative losses of carriers out off laser level 3 give a $\gamma = 1.8$ dependence. From Fig. 4 we find that R_{PP} dominates the total RIN for $P_0 < 2$ mW and the spontaneous emission is the main noise source. For $P_0 > 2$ mW, R_{33} is dominant and non-radiative losses of carriers out off the upper laser level are the main noise sources. The superposition of R_{PP} and R_{33} to the total RIN results in an effective power-law dependence of RIN on the optical power with $\gamma = 1.98$.

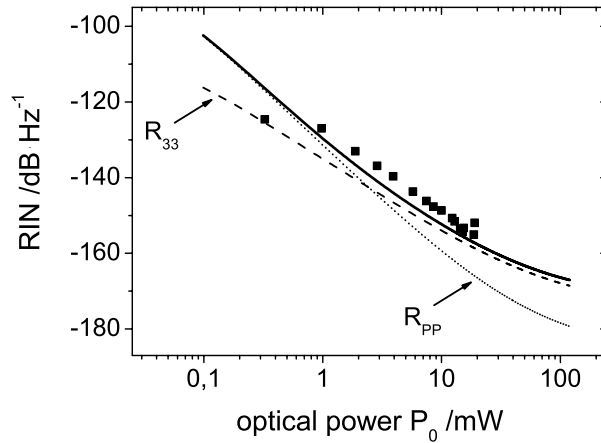


Fig. 4. Calculated relative intensity noise RIN as a function of the optical output power at a frequency of 40 MHz for the QC laser under investigation. The solid line shows the total RIN. Additionally, the individual contributions R_{PP} (dotted) and R_{33} (dashed) which give the main contribution to the RIN are indicated. The experimental RIN of Fig. 3 is also shown (squares) for comparison.

Table 1. Parameter values used for RIN calculations. The differential gain parameter is obtained by solving the steady-state rate equations and inserting the experimentally determined threshold current. The spontaneous emission parameter β is determined from a fit to the experimental PI-curve. The photon lifetime is obtained from the measurement of the net modal gain [18] and the phonon scattering times are estimated using Fermi's Golden rule for the intersubband transition [18].

parameter	symbol	value
differential gain parameter	g	$4.8 \times 10^4 \text{ s}^{-1}$
spontaneous emission factor	β	1×10^{-6}
photon lifetime	τ_P	4.3 ps
phonon scattering time (3 \rightarrow 2)	τ_{32}	2.1 ps
phonon scattering time (3 \rightarrow 1)	τ_{31}	2.6 ps
phonon scattering time (2 \rightarrow 1)	τ_{21}	0.3 ps

The good agreement between the experiment and the model gives us now the opportunity to study key features of the three-level scheme. So far, we have investigated the intensity noise properties of a three-level QC laser with $Z = 25$ gain stages incorporated into the active region. In the following we analyze the influence of the number of gain stages Z on the intensity noise of QC lasers. Therefore, we have first calculated the RIN for QC lasers with different numbers of gain stages incorporated into the active region. Then, we have analyzed the RIN with respect to the power scaling parameter γ at an injection current of $1.2I_{thr}$. We have performed these simulations keeping the differential gain parameter g constant. The results are depicted in Fig. 5. The power scaling parameter γ decreases with increasing number of gain stages incorporated

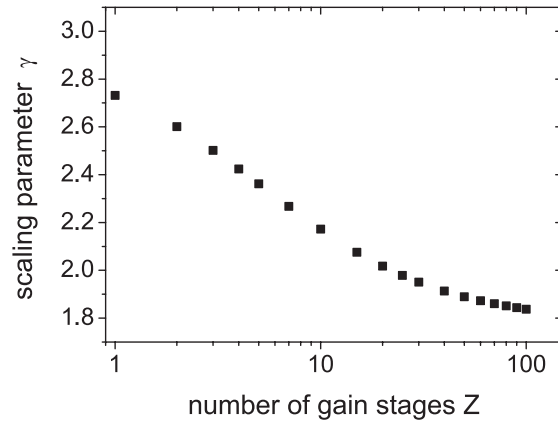


Fig. 5. Scaling parameter γ of the calculated RIN as a function of the number of gain stages Z incorporated into the active region of a QC laser at an injection current of $1.2I_{thr}$.

into the active region. For $Z = 1$, $Z = 25$, and $Z = 100$ we obtain $\gamma = 2.73$, $\gamma = 1.98$, and $\gamma = 1.84$, respectively. For large Z , the power scaling parameter γ levels on the value of $\gamma_3 = 1.8$. Hence, RIN can be approximated solely by R_{33} . On the other hand, RIN calculations for a QC laser with only one gain stage $Z = 1$ yield $\gamma = 2.73$ for the total RIN. Hence, QC lasers with a single gain stage active region show a similar noise behavior as conventional interband semiconductor lasers even though the non-radiative loss rate of carriers out off the upper laser level is about three orders of magnitude larger for QC lasers than for interband semiconductor lasers due to the shorter electron lifetime of the upper laser level which is \sim ps for QC lasers and \sim ns for interband semiconductor lasers, respectively. In this case the dominant part contributing to the RIN of QC lasers arises from R_{PP} , and the main noise source is the spontaneous emission. But, the influence of non-radiative losses of carriers out off the upper laser level on the RIN of QC lasers increases by cascading gain stages into the active region. The more gain stages are incorporated into the active region the stronger becomes the influence of R_{33} until it dominates the total RIN of QC lasers. Thus, the noise behavior of QC lasers depends on the number of gain stages cascaded into the active region.

In conclusion, we have investigated the intensity noise properties of 3-level QC lasers. We have analyzed the intensity noise in terms of the RIN. We measured the RIN of a QC laser in the low frequency limit at 40 MHz in cw operation at a heat sink temperature of 88 K. We find that RIN decreases with increasing optical power according to a power-law as $RIN \propto P_0^{-\gamma}$, with $\gamma \approx 2.1$. From a semiclassical noise model for a QC laser incorporating $Z = 25$ gain stages we find that $\gamma \approx 2$ is due to the cascaded gain stages. In this case, non-radiative losses of carriers out off the upper laser level become the dominant noise source. In contrast, for $Z = 1$ the spontaneous emission is the main noise source and $\gamma = 2.73$ is obtained. Thus, the power scaling behavior of the intensity noise of lasers possessing 3-level cascaded gain stages depends on the number of gain stages incorporated into the active region.

Acknowledgments

We would like to thank Dr. Ingo Fischer (Darmstadt University of Technology, now with Vrije Universiteit Brussel) and Dr. Thomas Beyer (Fraunhofer-IPM, Freiburg) for fruitful discussions and helpful suggestions. Funding of the present work by the German Federal Ministry of Education and Research (BMBF) under contract no. FKZ 13N8034 is gratefully acknowledged.